JACS
JOURNAL OF THE AMERICAN CHEMICAL SOCIETY

ARTICLE

pubs.acs.org/JACS

Enhancement of the Catalytic Activity of Supported Gold Nanoparticles for the Fenton Reaction by Light

Sergio Navalon,[†] Maykel de Miguel,[†] Roberto Martin,[†] Mercedes Alvaro,[†] and Hermenegildo Garcia[*,‡]

[†]Departamento de Química, Universidad Politécnica de Valencia, Camino de Vera s/n, 46022 Valencia, Spain

[‡]Instituto de Tecnología Química CSIC-UPV, Universidad Politécnica de Valencia, Av. De los Naranjos s/n, 46022 Valencia, Spain.

Supporting Information

ABSTRACT: Laser flash photolysis of supported gold nanoparticles exciting at the surface plasmon band (532 nm) has allowed in the case of Au/CeO_2 and Au/OH-npD (OH-npD: Fenton-treated diamond nanoparticles) detection of transients decaying in the microsecond time scale that have been attributed as indicating photoinduced electron ejection from gold based on N_2O quenching and the observation of the generation of methyl viologen radical cations. This photochemical behavior has led us to hypothesize that there could be assistance to the catalytic activity of these materials by irradiation in those cases wherein the mechanism involves electron transfer to or from a substrate to the gold. This hypothesis has been confirmed by observing that the catalytic activity of Au/OH-npD for the Fenton degradation of phenol with hydrogen peroxide can be increased over 1 order of magnitude by irradiation at 532 nm. Moreover, there is a linear relationship between the initial reaction rate and the incident photon flux. This photoenhancement allows promoting Fenton activity at pH 8 in which the catalytic activity of Au/OH-npD is negligible. The same photo enhancement activity for the Fenton degradation of phenol was observed for other supported gold catalysts including those that do not exhibit microsecond transients in the nanosecond laser flash photolysis (Au/TiO_2 and Au/SiO_2) due to their lifetime shorter than microseconds. It is proposed that the photo enhancement should be a general phenomenon in gold catalysis for those reaction mechanisms involving positive and/or negative gold species.

INTRODUCTION

The Fenton reaction consists in the generation of hydroxyl radicals by reduction of hydrogen peroxide with Fe^{2+} or other reducing transition metals.[1−4] The importance of the Fenton reaction derives from its general applicability to degrade organic pollutants present in soils and waters.[5−7] A remaining drawback of this process is the need of stoichiometric amounts of iron salts that are required to effect the generation of hydroxyl radicals. Development of heterogeneous catalysts that avoid the need of large amounts of reducing metal ions has been an active research front in this area. While there are many reports describing the use of iron-containing aluminosilicates as solid catalysts for the Fenton reaction, they typically use a large excess of hydrogen peroxide (above the stoichiometric amount by 100-fold), giving an idea of the efficiency level of these materials.[8−11] Considering that hydrogen peroxide is a relatively expensive commodity, development of efficient heterogeneous Fenton catalysts using a low hydrogen peroxide excess is still necessary in order to make the Fenton process affordable as a general decontamination/disinfection treatment. Recently we have reported that gold nanoparticles supported on modified diamond nanoparticles (Au/OH-npD) is an extremely efficient solid catalyst for the Fenton reaction, exhibiting turnover numbers as high as 320 000 cycles with a minimum selectivity toward hydroxyl radical generation of 79% of consumed hydrogen peroxide. The present work shows that upon illumination with light of the adequate wavelength Au/HO-npD becomes even more active and selective for the Fenton process, and under these conditions the catalyst can even operate at neutral or basic pH values, for which the Au/OH-npD is inactive in the dark. The photo enhancement observed for Au/HO-npD appears to be also present for other supported gold catalysts that increase their activity upon illumination. Evidence is presented suggesting that this photo enhancement can be a general phenomenon and could also operate in many other processes whose mechanism involves a step of electron transfer from gold to the substrate.

The photochemistry of gold nanoparticles either in colloidal solutions or supported on a solid has been a topic of much interest since the late 1990s.[12−17] Now there is a renewed interest on the photochemistry of supported gold nanoparticles in systems with low gold loading and supports that are relevant in heterogeneous gold catalysis.[18−20] Thus, although the photochemistry of gold nanoparticles supported on TiO_2 was the subject of pioneering studies by El-Sayed and Kamat,[12,17,21−23] the samples of these studies contained large nanoparticles around

Received: September 30, 2010
Published: January 31, 2011

dx.doi.org/10.1021/ja108816p | J. Am. Chem. Soc. 2011, 133, 2218–2226

40 nm and gold loadings over 20% and very frequently even about 50%. These Au/TiO_2 samples are much different from the current heterogeneous gold catalysts for which the tendency is to prepare materials at loadings even below 1% and particle size as small as possible, but certainly below 10 nm. The remarkable differences in gold loading and particle size have a strong influence on the photochemical processes taking place since at high loading agglomeration and particle growth is the main effect observed due to the thermal relaxation of the photon energy. Also recently we have shown that upon illumination with visible light Au/TiO_2 exhibits a remarkable photocatalytic activity that can be used for the degradation of deadly chemical warfare agents and for water splitting.[20] Thus, the previously observed photochemical processes such as particle size growth and change in the particle morphology reported for materials with large gold nanoparticles and high gold loadings are no longer observed for those gold materials having activity as solid catalysts. Therefore, a photochemical study on catalytically active supported gold materials is an interesting topic *per se* that can eventually lead to new findings of relevance in catalysis as does the one reported here.

In the present work we have performed an initial laser flash photolysis study of some widely used supported gold catalysts. From the detection of photogenerated transients and subsequent rationalization of the photochemical events, we have proposed that these systems should exhibit upon illumination an enhanced catalytic activity for those reactions in which the mechanism requires that gold activates the substrate by transferring electrons in the rate-determining step. The data that will be presented below provide evidence supporting this claim and open a new avenue for the assistance of catalytic reactions by irradiation at the wavelengths corresponding to the gold surface plasmon band.

RESULTS AND DISCUSSION

In the first stage of our work we selected a series of gold catalysts that have been frequently used in the literature to promote a wide range of organic reactions including aerobic oxidations, selective hydrogenations, and couplings among other reactions.[24−26]

Table 1 lists the catalysts under study, their gold content, average particle size, position of the surface plasmon band (λ_{SPB}), and key references in which these materials have been used. It should be remarked that in one case this gold catalyst is commercially available (Au/TiO_2) and constitutes a reference catalyst. Also, Au/CeO_2 consisting of gold nanoparticles (average size 2.3 nm) supported on nanoparticulated ceria (5 nm average diameter) prepared by hydrolysis of $Ce(NO_3)_4$ (see Supporting Information for synthetic details) is one of the most efficient solid catalysts for the low-temperature CO oxidation,[27] aerobic alcohol oxidation,[28] and carbamoylation of aromatic amines.[29] In the other three cases, the gold samples studied are exactly the same batches that had been used as catalysts in the articles cited in Table 1. The series also contains the newly reported Au/OH-npD that corresponds to the same batch as that whose catalytic activity was reported for the Fenton reaction. Thus, all the gold catalysts used are exactly the same batches as those reported to exhibit high catalytic activity in aerobic oxidations, selective hydrogenations, or Fenton chemistry. In view of the fact that all these catalysts have been thoroughly characterized in the literature, we provide in the present work only the pertinent new data (Table 1); however, comprehensive characterization data of these materials can be found in the cited literature. The reader is referred to these original reports for a detailed description of other data such as preparation procedures, XPS, surface area measurements, gold oxidation state, etc.

Table 1. Relevant Data of the Catalysts Used in This Work

catalyst	size[a] nm	loading wt %	λ_{SPB}[b] nm	refs
Au/CeO_2	<1	1	536	30
Au/TiO_2	8,5	1.5	565	31
Au/HO-npD	<1	1.0	535	32
Au/ZrO_2	5	1.5	539	33,34
Au/SiO_2	2.5	1.2	524	35

[a] Average particle size. [b] Position of the maximum absorption of surface plasmon band.

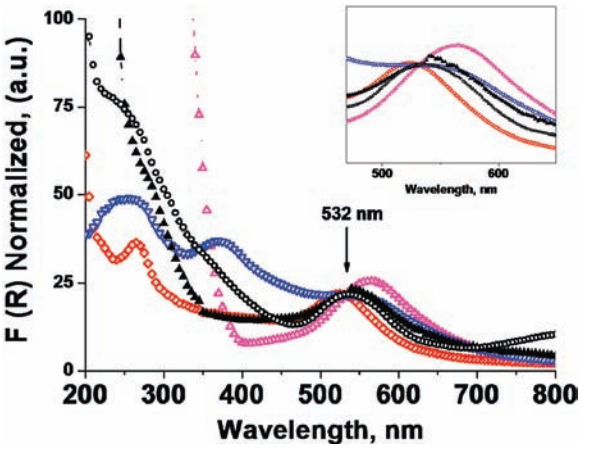

Figure 1. Diffuse reflectance UV/vis spectra (plotted as the Kubelka−Munk function of the reflectivity, *R*) normalized at 532 nm of the five supported gold catalysts used in the present study. (▲ [red]) Au/TiO_2, (◊ [red]) Au/SiO_2, (▼ [blue]) Au/CeO_2, (▲) Au/ZrO_2, and (○) Au/HO-npD. Inset shows a magnification of the 450−650 nm region.

It is pertinent to comment that all the samples consist of small gold nanoparticles at very similar low weight loading (see Table 1). These two characteristics are important distinctive features with respect to the materials whose photochemistry has been reported so far in the literature. In spite of the low loading, all the samples exhibit the characteristic surface plasmon band due to the presence of gold. Significant differences in the intensity, shape, width, and wavelength maximum of the corresponding surface plasmon band are observed from sample to sample due to some differences in sizes, shapes, content, dielectric constant of the support, and interaction of the gold nanoparticles with the support. Figure 1 shows the diffuse reflectance UV−vis spectra of the five samples under study. Importantly, all the samples exhibit light absorption at 532 nm due to gold, the wavelength of the laser used in the first part of this study. It should be commented, however, that gold clusters having less than 2 nm in diameter and being catalytically the most active species in thermal reactions do not exhibit generally intense surface plasmon band.[36] Thus, it may be that the most active nanoparticles for the thermal catalytic reactions are not exactly those that are going to be preferentially excited by irradiation at the gold surface plasmon band.

dx.doi.org/10.1021/ja108816p |*J. Am. Chem. Soc.* 2011, 133, 2218–2226

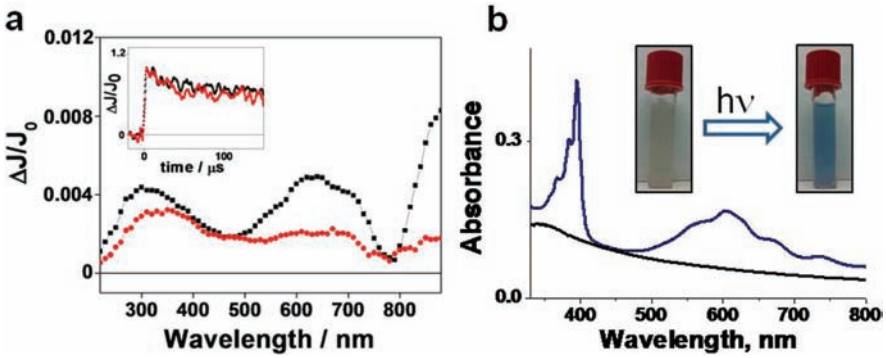

Figure 2. (a) Transient spectra recorded 3 μs after the 532 nm laser pulse for acetonitrile suspensions of Au/CeO_2 (0.5 mg mL^{-1}) under nitrogen (■) and oxygen (● [red]). The inset shows the comparison of the signal temporal profile recorded at 400 nm under N_2 and O_2. (b) UV−vis spectra of N_2-purged acetonitrile suspensions of Au/CeO_2 containing MV^{2+} before (black line) and after (blue line) irradiation at λ_{ex} = 532 nm. The blue color observed corresponds to the formation of $MV^{\bullet+}$.

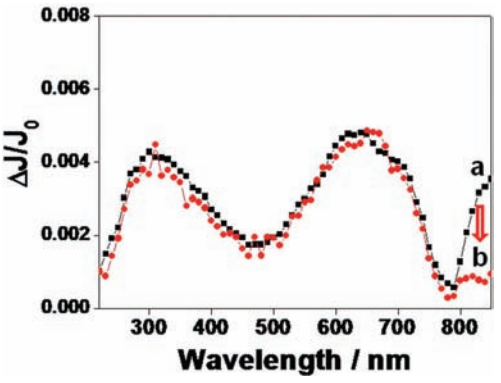

Figure 3. Transient spectra recorded at 3 μs after 532 nm laser excitation for an aqueous suspension of Au/CeO_2 under N_2 atmosphere (a) and saturated with N_2O (b). The arrow at 840 nm shows the disappearance of the absorption in this region due to the quenching of aquated electrons.

Preliminary studies were carried out using a nanosecond laser flash system exciting at 532 nm and detecting changes in the optical spectrum in the reflectance mode. No transient signals decaying in the nanosecond or longer time scales could be observed for Au/TiO_2, Au/ZrO_2, or Au/SiO_2. Probably in these three cases for which our nanosecond system does not detect any transient, the photochemical events occur in shorter time scales as it has been reported for Au/TiO_2,[13,16,21,22,37] and the photogenerated transient will go undetected in our nanosecond system. In particular, we do not observe the bleaching of the surface plasmon band reported for Au/TiO_2 occurring in the picoseconds time scale.[13,16,21,22,37]

In contrast to the behavior observed for the previous three gold samples, transient signals decaying in microsecond time scale were observed for Au/CeO_2 and Au/OH-npD. Figures 2 and 3 show the transient spectra recorded for acetonitrile suspensions of Au/CeO_2 and dry Au/HO-npD powders under nitrogen.

Importantly, both in the cases of Au/HO-npD and Au/CeO_2, photolysis of the supports lacking gold nanoparticles under the same conditions did not show any transient, thus proving that the transients derive from gold excitation with visible light.

We speculated that these transient spectra could be due, at least partly, to charge separated species. Photoinduced charge separation is a general phenomenon that has been observed for gold nanoparticles upon irradiation.[38,39] We know that laser flash photolysis of suspended solids is very uncommon due to a rapid deposition of the powders. However, the textural and physical properties of the nanoparticles that have been used herein and the fact that we are working with diluted suspensions allow the use of transmission spectroscopy, therefore increasing the quality of the spectra. Figure 2, corresponding to photolysis of Au/CeO_2, exhibits a local maximum above 900 nm. On the basis of the position of the band we speculated that this peak beyond 900 nm could correspond to solvated electrons.[40] Strong support for this assignment consistent with the position of the band was the fact that oxygen quenches the peak considerably. It is known that oxygen can trap electrons, forming superoxide and other reactive oxygen species.[41]

In order to demonstrate this hypothesis we performed a quenching study to prove photoinduced electron ejection which consisted in bubbling N_2O into an aqueous suspension of the material. This would lead to the quenching of the solvated electrons according to eq 1, quenching of the solvated electrons by N_2O in aqueous media.

$$e^-_{(aq)} + N_2O + H_2O \rightarrow HO^\bullet + HO^- + N_2 \qquad (1)$$

The results are shown in Figure 3. The band above 900 nm completely disappears when N_2O-saturated suspension of Au/CeO_2 is submitted to laser flash photolysis.

Photoinduced charge separation is a general phenomenon that has been observed for gold nanoparticles upon irradiation, and the presence[38,42] of solvated electrons in the photolysis of Au/CeO_2 is consistent with this process. Strong support to this assignment is provided by the fact that steady-state irradiation of acetonitrile suspensions of Au/CeO_2 or Au/HO-npD powders containing methyl viologen (MV^{2+}) gives rise to the characteristic blue color (see inset of Figures 2b and 4b) and corresponding optical spectrum of the expected $MV^{\bullet+}$ cation. Generation of the $MV^{\bullet+}$ cation can be rationalized considering that MV^{2+} is trapping photoejected electrons as depicted in Scheme 1 or is generated by strongly reducing gold species.

Photoassisted Catalytic Fenton Reaction. As we have commented in the Introduction, the series of materials under study are widely used catalysts for a large variety of processes.[25,26] We want to demonstrate that the proposed long-lived photoinduced charge separation can be useful to boost the catalytic activity of these materials upon illumination, particularly for the two catalysts that show detectable transients in the microsecond

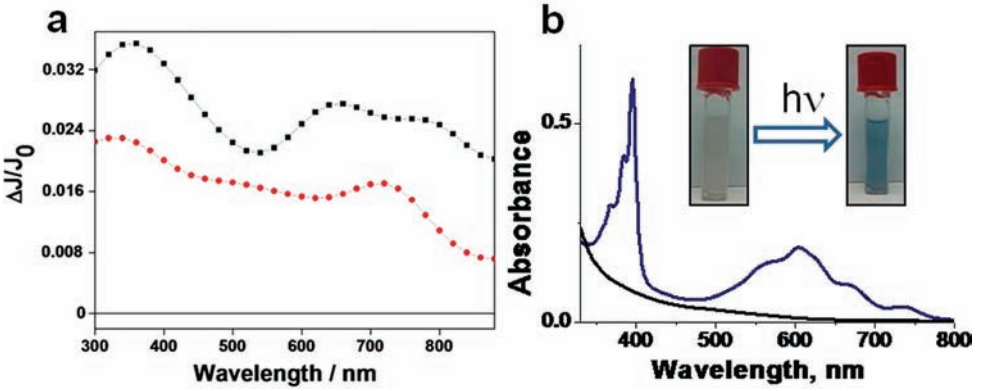

Figure 4. (a) Diffuse-reflectance transient spectra recorded 69 μs after the 532 nm laser pulse in solid state for Au/HO-npD under nitrogen (■) and oxygen (● [red]). (b) Steady-state UV−vis spectra of N_2-purged acetonitrile suspensions of Au/HO-npD containing MV^{2+} before (black line) and after (blue line) irradiation at λ_{ex} = 532 nm. The inset of part b shows a photograph of the cuvette before and after 532 nm irradiation whereby development of the blue color corresponding to the formation of $MV^{\bullet+}$ can be observed.

Scheme 1. Rationalization of the Formation of $MV^{\bullet+}$ Cation Considering That MV^{2+} Is Trapping Photoejected Electrons after 532 nm Laser Irradiation of Au/HO-npD or Au/CeO_2

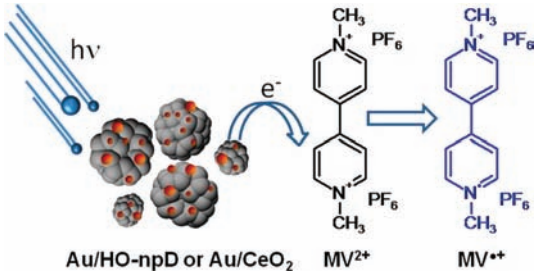

time scale. To prove this hypothesis and considering that $MV^{\bullet+}$ can be generated upon irradiation, we selected a reaction wherein the mechanism requires as the key step an electron transfer from gold to the substrate. For these processes, irradiation of the catalyst should be an effective way to promote the rate-determining step, and this could lead to an increase of the catalytic activity. The reaction selected has been the catalytic Fenton degradation of phenol by hydrogen peroxide.[8] In this process, as in the stoichiometric Fenton reaction, injection of one electron into hydrogen peroxide gives rise to the generation of hydroxyl radicals that are the aggressive reaction intermediate attacking phenol (Scheme 2, reduction semireaction). According to this Scheme, if light absorption produces photoejection of electrons and these electrons are trapped by hydrogen peroxide, an enhancement of the catalytic activity of the supported gold for the transformation of phenol into hydroquinone and catechol should be observed upon illumination on the gold surface plasmon band. In the subsequent step H_2O_2 should be able to reduce the oxidized gold to the initial state (oxidation semireaction), thus closing the catalytic cycle. In this mechanism the support of the gold nanoparticles will play several roles including stabilization of the required gold oxidation states controlling the redox potential and also allowing hydroxyl radicals to diffuse into the liquid phase. At least in the case of TiO_2 as support, it has been found that a hydroxyl radical can remain bonded to the solid surface, limiting its diffusion into the solution as free $HO^{\bullet}$.[8] In contrast, in the case of inert diamond nanoparticles it has been proposed that one of the key features of its high Fenton activity is

Scheme 2. Proposed Mechanism for the Photochemical Enhancement of the Fenton Catalysis

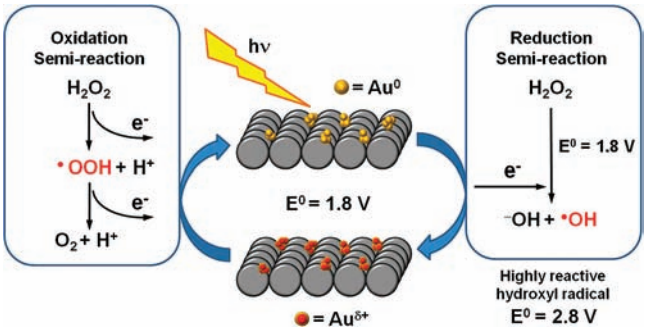

the inertness of the diamond surface, promoting the generation of free hydroxyl radicals. These considerations can explain why two materials, such as Au/HO-npD and Au/ZrO_2, having similar surface plasmon bands and therefore similar light absorption, exhibit greatly different enhancements upon the action of light, since the supports will favor the diffusion of •OH radicals (HO-npD) or will trap them (ZrO_2).

Our hypothesis was confirmed, and Figure 5 shows that 532 nm irradiation of Au/HO-npD suspended in an aqueous solution (pH 4) of phenol (100 mg L^{-1}) and hydrogen peroxide (200 mg L^{-1}) leads to a remarkable enhancement of the catalytic activity of Au/OH-npD. Both disappearance of phenol and decomposition of H_2O_2 undergo a significant enhancement upon irradiation at the gold surface plasmon band of the catalyst. Moreover, as it can be seen in Figure 5 the initial reaction rates, both for phenol and H_2O_2 disappearance, follow a linear relationship with the laser power (see Figure 6), thus indicating that the observed enhancement is due to the activation of light. Blank controls, irradiating a similar aqueous solution of phenol, H_2O_2, and npD in the absence of gold nanoparticles, do not show any promotion in the phenol or hydrogen peroxide disappearance by light, thus proving that gold is the actual species involved in the photoassistance.

Previous studies have shown that Au/OH-npD is already a highly efficient catalyst for the Fenton reaction at pH = 4. Thus, the new data presented here show that this catalytic activity already manifested in the dark can be enhanced even over 1 order

dx.doi.org/10.1021/ja108816p |J. Am. Chem. Soc. 2011, 133, 2218–2226

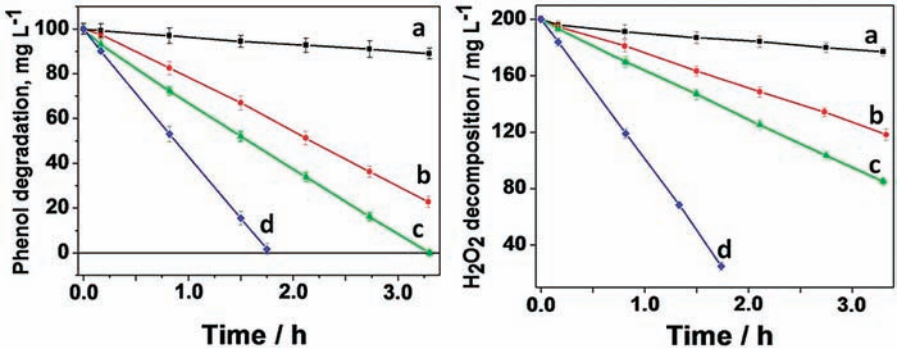

Figure 5. Influence of the laser intensity on the catalytic activity of Au/HO-npD for the Fenton reaction of phenol degradation (left) and H_2O_2 decomposition (right). Reaction conditions for phenol degradation using increasing laser powers. (a) 0 mJ pulse^{-1}, (b) 20 mJ pulse^{-1}, (c) 38 mJ pulse^{-1}, and (d) 70 mJ pulse^{-1}. Reaction conditions: 100 mg L^{-1} (1.06 mM) of phenol and 200 mg L^{-1} (5.88 mM) of H_2O_2 and Au/HO-npD 1.0% 160 mg L^{-1} (0.0056 mM) at pH = 4.

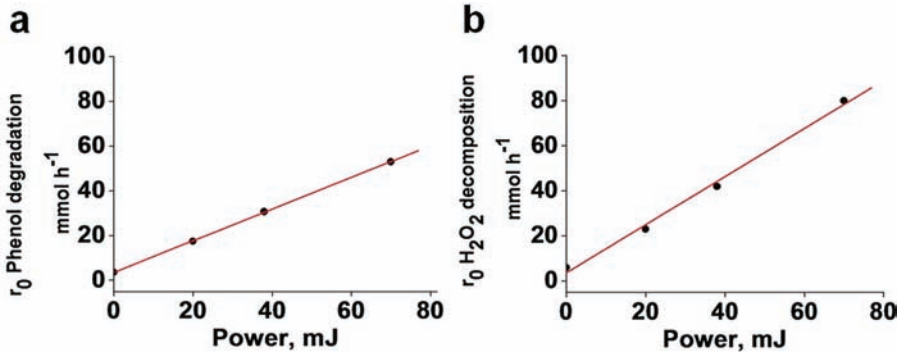

Figure 6. Linear relationship between the initial reaction rate and the laser power used for photochemical excitation: (a) for phenol degradation and (b) H_2O_2 decomposition in the presence Au/HO-npD catalyst. Reaction conditions: 100 mg L^{-1} (1.06 mM) of phenol and 200 mg L^{-1} (5.88 mM) of H_2O_2 and Au/HO-npD 1.0% 160 mg L^{-1} (0.0056 mM) at pH = 4.

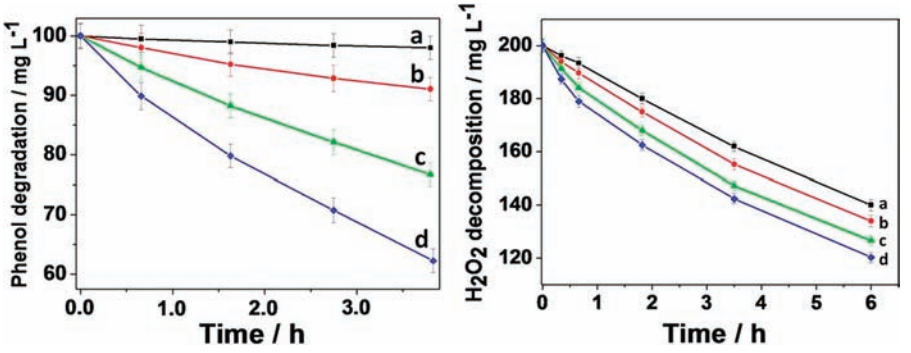

Figure 7. Influence of the laser power on the catalytic activity of Au/HO-npD for the Fenton reaction: determined as phenol disappearance (left) and H_2O_2 decomposition (right). (a) 0 mJ pulse^{-1}, (b) 20 mJ pulse^{-1}, (c) 38 mJ pulse^{-1}, and (d) 70 mJ pulse^{-1}. Reaction conditions: 100 mg L^{-1} (1.06 mM) of phenol and 200 mg L^{-1} (5.88 mM) of H_2O_2 and Au/HO-npD 1.0% 160 mg L^{-1} (0.0056 mM) at pH = 8.

of magnitude by irradiation into the gold surface plasmon band and that the process is monophotonic since it follows a linear relationship with the laser power (see Figure 6).

Besides laser excitation we also used solar light to irradiate the system. The same effect was observed, showing that the photochemical enhancement of the catalytic activity is a general phenomenon that does not need monochromatic laser excitation to occur.

The greatest interest of our findings would be to use the promotional effect of light to introduce new catalytic activity that does not occur in the dark. Since the Fenton reaction strongly depends on the pH, we have reported that no catalytic activity occurs at room temperature for Au/HO-npD at pH values above 5. This is a strong limitation since for general water treatment disinfection it would be highly desirable to have catalytic activity at quasi-neutral pH. Therefore, it was of interest to determine if irradiation of Au/OH-npD can promote the Fenton reaction that is not observed in the dark at pH 8. Figure 7 shows the temporal profile of phenol concentration and H_2O_2 concentration when the reaction is carried out at pH 8 using different laser powers.

dx.doi.org/10.1021/ja108816p |*J. Am. Chem. Soc.* 2011, 133, 2218–2226

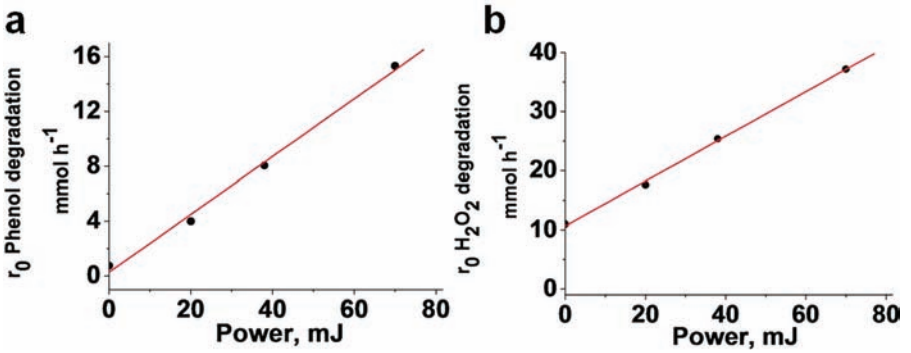

Figure 8. Linear relationship between the initial reaction rate and (a) the increasing laser power for phenol and (b) H_2O_2 degradation using Au/HO-npD catalyst. Reaction conditions: 100 mg L^{-1} (1.06 mM) of phenol and 200 mg L^{-1} (5.88 mM) of H_2O_2 and Au/HO-npD 1.0% 160 mg L^{-1} (0.0056 mM) at pH = 8.

As can be seen in this figure, in the absence of irradiation no phenol degradation occurs even though hydrogen peroxide is spuriously decomposed to oxygen under these basic conditions. In contrast, upon irradiation phenol degradation starts to occur at pH 8, and the initial reaction rate as well as final conversion increases linearly with the laser power (see Figure 8). Interestingly, the initial reaction rate of phenol disappearance at pH 8 can be enhanced over 1 order of magnitude when the irradiation is carried out at the maximum laser power. A similar trend is observed for the temporal profiles of hydrogen peroxide decomposition.

The linear dependence of the initial reaction rate for phenol disappearance with the laser power at either pH 4 or pH 8 (Figures 6 and 8, respectively), even though in both cases the monophotonic nature of the photochemical process exhibits a different slope of 0.86 and 0.23 mmol h^{-1} mJ^{-1}, respectively, indicating that the photoenhancement is larger at acid pH values. However, as remarkable as the difference in slope is, the fact is that at pH 8 no Fenton reaction was taking place in the dark.

In order to find conclusive evidence for the occurrence of the Fenton reaction under neutral conditions, EPR spectroscopy using phenyl *N-tert*-butyl nitrone (PBN) as spin trap to detect $OH^{\bullet}$ in aqueous solution at neutral pH was carried out. Controls in the dark showed that Au/HO-npD promotes under these conditions the formation of the OH-PBN adduct. Similarly, when Au/OH-npD, hydrogen peroxide, and PBN spin trap were illuminated with visible light. a well-resolved EPR signal corresponding to the trapping of $OH^{\bullet}$ is clearly observed. Other controls such as monitoring the EPR of H_2O_2 and PBN under illumination or irradiation or Au/HO-npD and PBN did not allow recording the spectrum of the HO-PBN adduct. Figure 9 shows EPR spectra recorded in the dark and upon illumination compared to the spectrum when the classical Fenton system (Fe^{2+} and H_2O_2) is used.

After having conclusively shown that light promotes the Fenton reaction using Au/OH-npD, we expanded the results to Au/CeO_2 that also exhibits microsecond transients in the laser flash photolysis. The results are shown in Figure 10.

As it can be seen, the main difference with Au/OH-npD and Au/CeO_2 is that in the dark the latter decomposes spuriously most of the hydrogen peroxide even at pH 4 without effecting phenol degradation. In other words, the efficiency of Au/CeO_2 as a Fenton catalyst in the dark is more than 10 times lower than that of Au/OH-npD. This remarkable lower efficiency of Au/

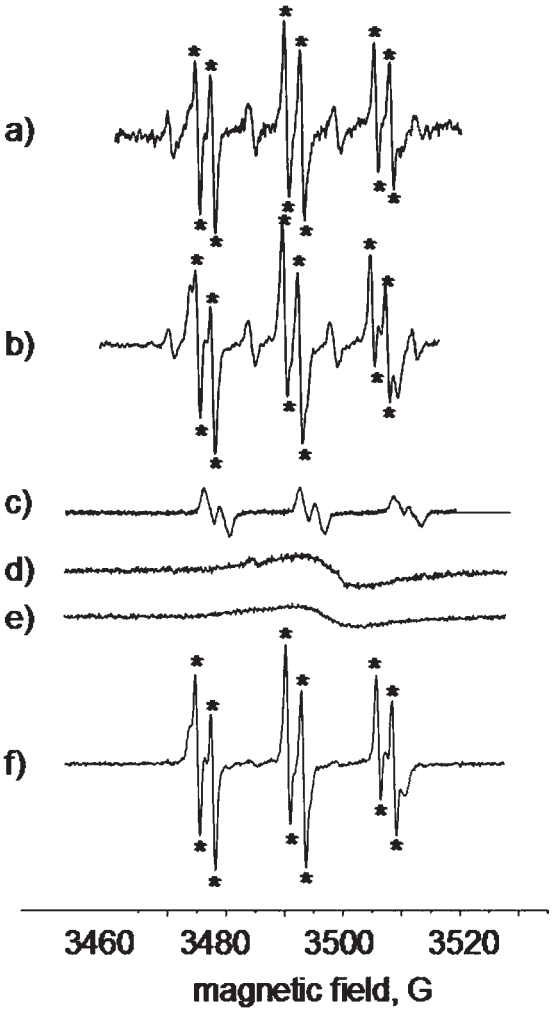

Figure 9. EPR spectra of (a) Au/HO-npD + H_2O_2 +PBN in the dark; (b) Au/HO-npD + H_2O_2 + PBN + 532 nm; (c) H_2O_2 +PBN; (d) Au/HO-npD +PBN; (e) Au/HO-npD; (f) classical Fenton system + PBN.

CeO_2 as a Fenton catalyst with respect to that of Au/HO-npD has already been reported in the literature.[8] However, even though Au/CeO_2 is a much less efficient catalyst for the Fenton reaction, the same effect of light promoting the generation of a hydroxyl radical leading to phenol degradation was again observed.

dx.doi.org/10.1021/ja108816p |*J. Am. Chem. Soc.* 2011, 133, 2218–2226

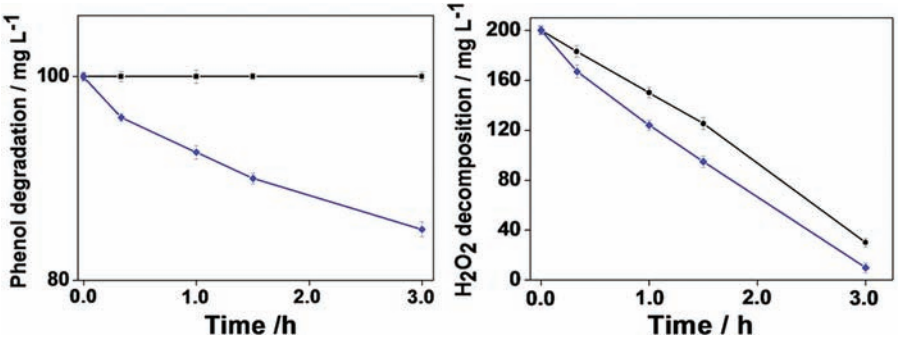

Figure 10. Degradation of phenol (left) and H_2O_2 (right) using (■) Au/CeO_2 catalyst at pH = 4 for the dark process and using (♦ [blue]) the maximum power employed in this study (70 mJ pulse^{-1}) for 532 nm laser excitation. Reaction conditions: 100 mg L^{-1} (1.06 mM) of phenol and 200 mg L^{-1} (5.88 mM) of H_2O_2 and Au/CeO_2 1.0% 160 mg L^{-1} (0.0056 mM) at pH = 4.

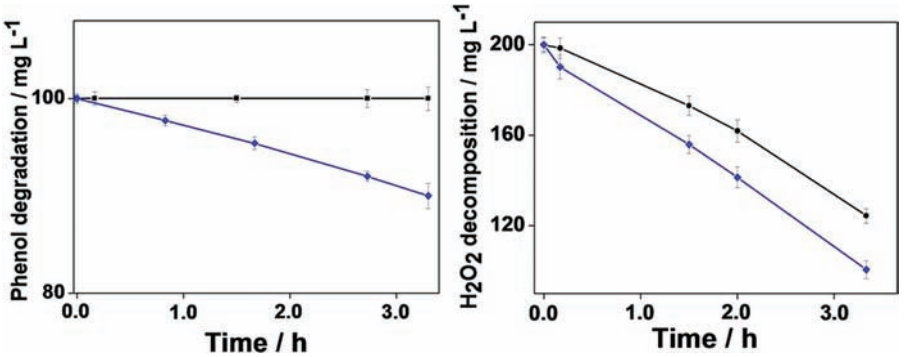

Figure 11. Degradation of phenol and H_2O_2 using Au/TiO_2 catalyst at pH = 4 for (■) blank and using the maximum power employed in this study (70 mJ pulse^{-1}) for (♦ [blue]) 532 nm laser excitation. Reaction conditions: 100 mg L^{-1} (1.06 mM) of phenol and 200 mg L^{-1} (5.88 mM) of H_2O_2 and Au/TiO2 1.0% 160 mg L^{-1} (0.0056 mM) at pH = 4.

As we have shown earlier, there are some supported gold catalysts that did not exhibit transients in the laser flash photolysis study. Particularly for Au/TiO_2 other transients have been detected at a much shorter time scale. Therefore, we speculated that the same photoinduced charge separation that has been observed for Au/OH-npD and Au/CeO_2 could be general for most of the supported catalysts except that the transient decays would be much faster than for Au/CeO_2 or Au/OH-npD and will be undetectable with our nanosecond system. If this were the case, then it could be possible that, even though no transients are observed in laser flash, improvements in the catalytic activity could still occur. Here we note again that the catalytic activity of the series of supported gold catalysts is much lower than that of Au/HO-npD. The enhancement of the Fenton activity by irradiation was checked with two gold catalysts, namely Au/TiO_2 and Au/SiO_2. The results for Au/TiO_2 are shown in Figure 11. As commented previously in the case of Au/CeO_2, Au/TiO_2 and Au/SiO_2 are poor Fenton catalysts in the dark compared to the very efficient Au/HO-npD. Thus, in the dark, spurious decomposition of H_2O_2 to O_2 and H_2O without leading to phenol degradation even at pH 4 occurs with these catalysts. However, even in these cases, the catalytic activity both for phenol degradation and H_2O_2 consumption increased when the samples were submitted to laser irradiation (see Figure 11 for the case of Au/TiO_2).

Overall, the results shown in Figures 5, 7, 10, and 11 show that irradiation of supported gold nanoparticles enhance their activity as Fenton catalysts. We have rationalized these results as arising from photoinduced electron ejection and charge separation. One alternative possibility to explain the previous results could be that gold nanoparticles convert the energy of the light into local heat that could promote the thermal cleavage of H_2O_2. However, although this possibility cannot be conclusively ruled out, it seems less likely than our proposal based on photoinduced electron injection supported by the observation of N_2O quenching and $MV^{\bullet+}$. The reason for this preference on the photoinduced electron injection over local heating is because increasing temperature of the reaction affects negatively the efficiency of the Fenton reaction that, in any case (either through photoinduced or thermal), would require single-electron reduction of H_2O_2 in order to generate hydroxyl radicals.

■ CONCLUSION

The present result clearly shows that the catalytic activity of supported gold nanoparticles as Fenton catalysts is promoted by irradiation of gold on the surface plasmon band either with monochromatic light or even with solar light. On the basis of the detection of photoinduced electron ejection, the experimentally observed catalytic enhancement can be attributed to the transfer of electrons from gold to hydrogen peroxide promoted by light. This effect is general regardless of the dark activity of the material. We have taken advantage of this photoassisted catalytic enhancement to carry out the Fenton reaction at moderate basic pH, conditions in which the dark catalytic process does not take place.

It can be anticipated that photoassistance phenomena observed here is much more general in gold catalysis than just the promotion of the Fenton reaction since the accepted mechanistic data for some gold-catalyzed reactions indicate the importance of positive and negative gold species as active sites in many reactions and electron transfer is a general step in many mechanisms. Thus, our findings open new avenues in gold catalysis by using light to promote the catalytic activity not observed in the dark.

EXPERIMENTAL SECTION

Gold Catalyst Preparation. *Au/HO-npD.* Au/HO-npD was obtained from commercial diamond nanoparticles (Aldrich) previously treated with H_2O_2 and $FeSO_4 \cdot 7H_2O$ in sulphuric acid. Au was deposited on HO-npD using $HAuCl_4 \cdot 3H_2O$ (800 mg) in 160 mL of deionized water brought to pH 9 by addition of 0.1 M aqueous NaOH solution. Once the pH value was stable, the solution was added to colloidal HO-npD (4.0 g) in H_2O (50 mL). After adjusting the pH at 9 (NaOH 0.1 M), the slurry was vigorously stirred for 18 h at room temperature. Au/HO-npD was then dispersed in distilled water and washed by performing five consecutive centrifugation−redispersion cycles with Milli-Q water. Au/HO-npD was dried under vacuum at room temperature for 1 h. Then 150 mg of Au/HO-npD was placed in a quartz reactor and submitted to H_2 reduction at 300 °C for 6 h. The total Au content of Au/HO-npD was 1 wt % as determined by chemical analysis.

The other catalysts were prepared as described in the Supporting Information.

Catalytic Tests. A quantity of Milli-Q water (100 mL) containing 100 mg L^{-1} (1.06 mM) of phenol and 200 mg L^{-1} (5.88 mM) of H_2O_2, and Au/HO-npD 1.0% 160 mg L^{-1} (0.0056 mM) was prepared and placed in an Erlenmeyer flask. The initial pH was adjusted to the required value, and the corresponding catalyst (H_2O_2 to metal molar ratio: 2318) was added, and the suspension was stirred in the dark. The time conversion was determined by analyzing aliquots (2 mL, filtered through 0.2 μm Nylon filter) by reverse-phase Kromasil-C18 column using H_2O/MeOH/acetic acid, 69:30:1, as eluent under isocratic conditions and a UV detector (monitoring wavelength 254 nm). The residual H_2O_2 was determined by 10-fold dilution of the reaction mixture and using $K_2(TiO)(C_2O_4)_2$ (Aldrich) in H_2SO_4/HNO_3 as colorimetric titrator. The solution was allowed to react for 10 min before monitoring at 420 nm.

Laser Flash Photolysis. Laser flash photolysis experiments were carried out in a Luzchem nanosecond laser flash system using the second (532 nm) harmonic of a Q-switched Nd:YAG laser for excitation (pulse ≤4 ns) and a 175 W ceramic Xenon Fiberoptic Lightsource, Cermax, perpendicular to the laser beam, as a probing light. The signal from the monochromator/photomultiplier detection system was captured by a Tektronix TDS 3032B digitizer. Laser system and digitizer are connected to a PC computer via GPIB and serial interfaces that controlled all the experimental parameters and provided suitable processing and data storage capabilities. The software package has been developed in the LabVIEW environment from National Instruments and compiled as a stand-alone application. The samples contained in Suprasil quartz 0.7 mm × 0.7 mm cuvettes capped with septa were purged with a N_2 or O_2 flow at least 15 min before the laser experiments.

ASSOCIATED CONTENT

Supporting Information. Synthetic details and relevant characterization data for all the catalysts used in this study. This material is available free of charge via the Internet at http://pubs.acs.org.

AUTHOR INFORMATION

Corresponding Author
hgarcia@qim.upv.es

ACKNOWLEDGMENT

Financial support by Spanish MICINN (CTQ2009-11583) is grateful acknowledgment. S.N. thanks the Technical University of Valencia for an assistant professor contract (Programa Cantera). R.M. thanks Spanish minister of Science Innovation MICINN for a FPU postgraduate fellowship.

REFERENCES

(1) Gogate, P. R.; Pandit, A. B. *Adv. Environ. Res.* **2004**, *8*, 501–551.
(2) Gogate, P. R.; Pandit, A. B. *Adv. Environ. Res.* **2004**, *8*, 553–597.
(3) Neyens, E.; Baeyens, J. *J. Hazard. Mater.* **2003**, *98*, 33–50.
(4) Pignatello, J. J.; Oliveros, E.; MacKay, A. *Crit. Rev. Environ. Sci. Technol.* **2006**, *36*, 1–84.
(5) Watts, R. J.; Dilly, S. E. *J. Hazard. Mater.* **1996**, *51*, 209–224.
(6) Pera-Titus, M.; Garcia-Molina, V.; Banos, M. A.; Gimenez, J.; Esplugas, S. *Appl. Catal., B* **2004**, *47*, 219–256.
(7) Chamarro, E.; Marco, A.; Esplugas, S. *Water Res.* **2001**, *35*, 1047–1051.
(8) Navalon, S.; Alvaro, M.; Garcia, H. *Appl. Catal., B* **2010**, *99*, 1–26.
(9) Caudo, S.; Centi, G.; Genovese, C.; Perathoner, S. *Appl. Catal., B* **2007**, *70*, 437–446.
(10) Centi, G.; Perathoner, S.; Torre, T.; Verduna, M. G. *Catal. Today* **2000**, *55*, 61–69.
(11) Perathoner, S.; Centi, G. *Top. Catal.* **2005**, *33*, 207–224.
(12) Link, S.; Burda, C.; Mohamed, M. B.; Nikoobakht, B.; El-Sayed, M. A. *J. Phys. Chem. A* **1999**, *103*, 1165–1170.
(13) Fujiwara, H.; Yanagida, S.; Kamat, P. V. *J. Phys. Chem. B* **1999**, *103*, 2589–2591.
(14) Kamat, P. V.; Flumiani, M.; Hartland, G. V. *J. Phys. Chem. B* **1998**, *102*, 3123–3128.
(15) Lahiri, D.; Subramanian, V.; Shibata, T.; Wolf, E. E.; Bunker, B. A.; Kamat, P. V. *J. Appl. Phys.* **2003**, *93*, 2575–2582.
(16) Subramanian, V.; Wolf, E.; Kamat, P. V. *J. Phys. Chem. B* **2001**, *105*, 11439–11446.
(17) Vinodgopal, K.; Bedja, I.; Kamat, P. V. *Chem. Mater.* **1996**, *8*, 2180–2187.
(18) Buso, D.; Pacifico, J.; Martucci, A.; Mulvaney, P. *Adv. Funct. Mater.* **2007**, *17*, 347–354.
(19) Carneiro, J. T.; Yang, C.-C.; Moma, J. A.; Moulijn, J. A.; Mul, G. *Catal. Lett.* **2009**, *129*, 12–19.
(20) Neatu, S.; Cojocaru, B.; Parvulescu, V. I.; Somoghi, V.; Alvaro, M.; Garcia, H. *J. Mater. Chem.* **2010**, *20*, 4050–4054.
(21) Dawson, A.; Kamat, P. V. *J. Phys. Chem. B* **2001**, *105*, 960–966.
(22) Jakob, M.; Levanon, H.; Kamat, P. V. *Nano Lett.* **2003**, *3*, 353–358.
(23) Kamat, P. V. *Langmuir* **1985**, *1*, 608–11.
(24) Stephen, A.; Hashmi, K.; Hutchings, G. J. *Angew. Chem., Int. Ed.* **2006**, *45*, 7896–7936.
(25) Hashmi, A. S. K. *Chem. Rev.* **2007**, *107*, 3180–3211.
(26) Corma, A.; Garcia, H. *Chem. Soc. Rev.* **2008**, *37*, 2096–2126.
(27) Carrettin, S.; Concepcion, P.; Corma, A.; Lopez Nieto, J. M.; Puntes, V. F. *Angew. Chem., Int. Ed.* **2004**, *43*, 2538–2540.
(28) Abad, A.; Concepcion, P.; Corma, A.; Garcia, H. *Angew. Chem., Int. Ed.* **2005**, *44*, 4066–4069.
(29) Juarez, R.; Concepcion, P.; Corma, A.; Fornes, V.; Garcia, H. *Angew. Chem., Int. Ed.* **2010**, *49*, 1286–90.
(30) Abad, A.; Corma, A.; Garcia, H. *Chem.—Eur. J.* **2008**, *14*, 212–222.
(31) Carrettin, S.; Hao, Y.; Aguilar-Guerrero, V.; Gates, B. C.; Trasobares, S.; Calvino, J. J.; Corma, A. *Chem.—Eur. J.* **2007**, *13*, 7771–7779.

(32) Navalon, S.; Martin, R.; Alvaro, M.; Garcia, H. *Angew. Chem., Int. Ed.* **2010**, *49*, 8403–8407.
(33) Azizi, Y.; Pitchon, V.; Petit, C. *Appl. Catal., A* **2010**, *385*, 170–177.
(34) Wu, H.; Shuai, Q.; Zhu, Z.; Hu, S. *Adv. Mater. Res. (Zürich.)* **2010**, 21–27.
(35) Kirichenko, O. A.; Kapustin, G. I.; Nissenbaum, V. D.; Tkachenko, O. P.; Poluboyarov, V. A.; Tarasov, A. L.; Kucherov, A. V.; Kustov, L. M. *Stud. Surf. Sci. Catal.* 537−540.
(36) Shimizu, T.; Teranishi, T.; Hasegawa, S.; Miyake, M. *J. Phys. Chem. B* **2003**, *107*, 2719–2724.
(37) Kamat, P. V. *Chem. Rev.* **1993**, *93*, 267–300.
(38) Aprile, C.; Herranz, M. A.; Carbonell, E.; Garcia, H.; Martin, N. *Dalton Trans.* **2009**, *1*, 134–139.
(39) Alvaro, M.; Aprile, C.; Ferrer, B.; Sastre, F.; Garcia, H. *Dalton Trans.* **2009**, *36*, 7437–7444.
(40) Murov, S. L., *Handbook of Photochemistry*; Marcel Dekker: New York, 1973; p 272.
(41) Martin, R.; Jimenez, L. B.; Alvaro, M.; Scaiano, J. C.; Garcia, H. *Chem.—Eur. J.* **2009**, *15*, 8751–8759.
(42) Primo, A.; Corma, A.; Garcia, H. *Phys. Chem. Chem. Phys.* **2011**, *13*, 866–910; 10.1039/c0cp00917b.